

Electromagnetic constraints on strike-slip fault geometry—The Fraser River fault system

Alan G. Jones, Ron D. Kurtz, David E. Boerner, James A. Craven, Gary W. McNeice
Geological Survey of Canada, 1 Observatory Crescent, Ottawa, Ontario K1A 0Y3, Canada

D. Ian Gough

Department of Physics, University of Alberta, Edmonton, Alberta T6G 2J1, Canada

Jon M. DeLaurier

Geological Survey of Canada, Pacific Geoscience Centre, Sidney, British Columbia V8L 4B2, Canada

Rob G. Ellis

Department of Geophysics and Astronomy, University of British Columbia, Vancouver, British Columbia V6T 1Z4, Canada

ABSTRACT

Magnetotelluric data from four profiles crossing the Eocene strike-slip Fraser River fault in southwestern British Columbia suggest that it penetrates the entire crust. This conclusion is supported by seismic reflection observations of a 2–3 km step in the Moho slightly to the east of the surface expression of the fault, but is at variance with an interpretation of the seismic data in which the fault soles into mid-crustal reflectors that seem to be continuous across the fault trace. A crustal-penetrating geometry supports the proposal that the Fraser River fault forms part of a 2500-km-long intracontinental transform fault system in northwestern North America. Modeling studies resolve a thin, highly conducting mid-crustal zone that is connected electrically to the conducting lower crust beneath the Coast belt. Low $\delta^{13}\text{C}$ values close to the Fraser fault system suggest that the electromagnetic signature of this zone may be due to the presence of organic carbon.

INTRODUCTION

Geological and geophysical studies over the past 30 years have been conducted to determine the geometry of major subvertical strike-slip fault zones at depth. Four generic geometries below the Conrad in the ductile lower crust are proposed (Fig. 1): downward continuation of the narrow fault zone into an equally narrow quasi-plastic shear zone (A in Fig. 1), downward continuation of the narrow fault zone into a zone with increasing breadth in the lower crust (B), decoupling of the steep fault zone into a wide zone of subhorizontal shear (C), and two narrow zones, one in the upper crust and one in the lower crust, connected by a narrow zone of subhorizontal detachment (D) (McGeary, 1989).

Difficulties with seismically imaging steeply dipping faults may have

caused prevailing thought to be biased against geometries A, B, and D in favor of geometry C. For four major faults, the San Andreas (Lemiszki and Brown, 1988, and references therein), the Great Glen–Walls Boundary (McGeary, 1989), the Dover (Keen et al., 1986), and the Bray–Vittel (Bois et al., 1986) faults, changes in reflection character at the base of the crust and diffractions from Moho offsets are considered evidence for their crustal extent. Lemiszki and Brown (1988) discussed the variability of strike-slip fault geometries and concluded that continental transform faults have a near-vertical crustal-penetrating nature (A, B, or D) in contrast to intra-plate strike-slip fault systems that are decoupled in the middle crust by subhorizontal detachments (C).

Deeply penetrating fault zones are significant for large-scale fluid circulation in the crust. McCaig (1988) and Nesbitt and Muehlenbachs (1989) have discussed circulation of surface-derived meteoric fluids deep within the crystalline crust (>10 km to as much as 25 km). Comparison of δD ratios for vein-forming fluids from the Rocky Mountain and Omineca belts was interpreted by Nesbitt and Muehlenbachs (1989) as indicative of metamorphic fluids in the former and meteoric fluids in the latter. The Fraser River fault is a candidate for either deep penetration of surface fluids or for escape of these fluids or fluids derived from metamorphic devolatilization from the lower crust.

Several first-order questions must be addressed for the Fraser River fault: (1) To what depth does the fault penetrate? (2) What is the geometry of the fault zone? (3) Is there an expression of the fault in the ductile lower crust? (4) Is the fault zone a conduit for fluids from the deep crust?

GEOLOGIC SETTING

The Fraser River fault (Fig. 2) is a major strike-slip vertical fault of late Eocene age (46.5–34 Ma; Coleman and Parrish, 1991). It cuts acutely across the north-northwest regional grain, dextrally offsetting rock units and their bounding faults, including the middle Eocene dextral strike-slip Yalakom–Hozameen fault, by ~100 km (Coleman and Parrish, 1991). To the east of the fault is the Intermontane superterrane, to the west is the Coast belt of the Insular superterrane (Fig. 2), and between it and the Yalakom fault lies Stikine terrane of oceanic affinity. At the surface the Yalakom fault has a northeasterly dip of 40°–60° in the region of Figure 1, steepening to a nearly vertical orientation further northwest (Coleman and Parrish, 1991). Crustal thickness in the region is estimated to be ~34 km from the recent seismic reflection data (Varsek et al., 1992).

The Fraser River fault and its southerly extension in the state of Washington, the Straight Creek fault, extend in a north-south direction for at least 500 km. Price and Carmichael (1986) suggested that the Fraser River–Straight Creek fault is the southern segment of a 200-km-long intracratonic transform fault system that includes the Tintina–northern Rocky Mountain trench fault zone. This view has been challenged by Coleman and Parrish (1991), who preferred to take up the Tintina–northern Rocky Mountain trench displacements on the Yalakom–Hozameen fault. Although the Fraser River fault is a major horizontal feature, there is

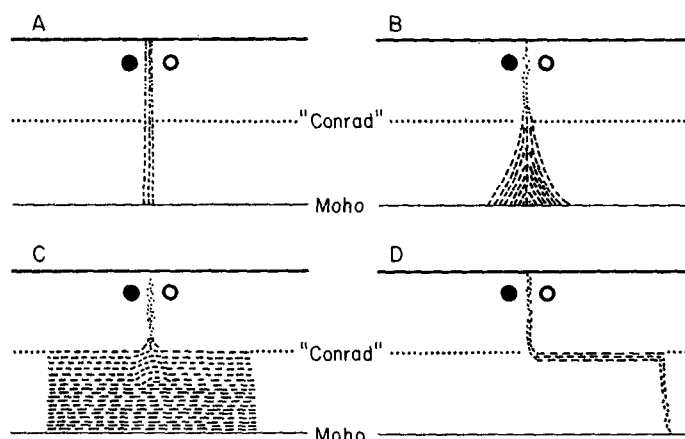


Figure 1. Four possible geometries for vertical strike-slip faults in ductile lower crust (based on McGeary, 1989).

no more than 3 km maximum vertical displacement in the region depicted by Figure 2 (J. Monger, 1990, personal commun.).

SEISMIC IMAGES

In 1988 seismic reflection data were acquired from Arrow Lake to the coast, and one of the profiles (line 18, Fig. 2) crossed the Fraser River fault (Varsek et al., 1992). Due to its vertical nature the Fraser River fault cannot be imaged directly by the seismic data, but differences in structural style of the reflections down to 6.3 s TWT (two-way traveltime) indicate its presence. At 6.3 s TWT, ~20 km, there is a band of flat-lying reflectors across the whole profile. Within the lower crust there is again a difference in structural style on either side of the surface location of the fault, with moderately east-dipping structures to the west but gently west-dipping structures, tapering into the Moho, to the east. At Moho depths there is a step change in crustal thickness of ~2 km west-side-down displacement just to the east of the surface trace of the fault.

Varsek et al. (1992) have considered three possible geometries for the fault; essentially A, B, and C of Figure 1. Their preference is for geometry C because of the 6.3 s reflective band and because the Yalakom and Hozameen faults appear to flatten into the mid-crust on profile 18 and on COCORP profile W7 in northern Washington State. Also, the Moho offset on line 18, when connected to a similar Moho offset seen on W7, has a different trend from the fault and is spatially related to extensional faults bounding the eastern Coast belt.

ELECTROMAGNETIC IMAGES

Electromagnetic (EM) studies are sensitive to changes in electrical conductivity. The depth and distance of investigation are governed by the skin-depth effect by which high frequencies (short periods) are most sensitive to the conductivity distribution close to the site, whereas low frequencies (long periods) sample the distant conductivity distribution. The magnetotelluric (MT) method uses Earth's natural time-varying EM fields, and surface measurements are made of the three magnetic components and the two horizontal electric components. Four MT profiles cross the Fraser River fault system in southwestern British Columbia (Fig. 2) and are separated by ~275 km along strike.

Induction Arrows

An indicator of structure, which has been used successfully to map many geologic and tectonic features, is induction, or "Parkinson," arrows

(Parkinson, 1959). These arrows display graphically the complex ratio between the vertical and horizontal magnetic components, and usually point toward regions of enhanced conductivity. The real arrows, at the period of maximum response to the fault (3.5 s, equivalent to mid-crustal depths), are illustrated in Figure 3. Currents flowing in the fault obviously vary with lateral distance along strike.

On profile *cb*, the reversal in direction of the arrows for sites 09 and 10 suggest that the current is preferentially flowing between these sites, although both are to the east of the Fraser River. A reversal is also apparent between sites 07 and 08 because of current flowing along the Yalakom fault (Fig. 2).

On *ewn*, the arrows in the vicinity of the fault system point northward and are an expression of the divergence of current due to the bifurcation of the two faults.

On *118*, the current is highly concentrated in the middle of the profile (see enlargement). The arrows are indicative of a simple two-dimensional conductivity structure.

On the southernmost profile, *ews*, the arrows are reversed about the fault and there is a reversal between stations 21 and 22 due to current flowing in the Pasayten fault.

Phase Pseudosections

An informative display of the MT data is a phase pseudosection; a contoured section of phase with distance along the abscissa and log(period) down the ordinate. A logarithmic scale is appropriate because of the exponential decay nature of EM fields with depth. The MT phase is 45° for a uniform zone, and phases greater than 45° indicate penetration into a zone of higher conductivity than the one above it, whereas phases less than 45° indicate penetration into a zone of less conductivity. The existence and location of major anomalies and the regional conductivity structural variations can be deduced from phase pseudosections.

The phases displayed here (Fig. 4) are the "effective" phases of the MT impedance tensor which have several appealing properties. Note that whereas the three southern profiles are east-west, the *cb* profile strikes N40°E, and accordingly there is stretching of the horizontal scale compared to the other three.

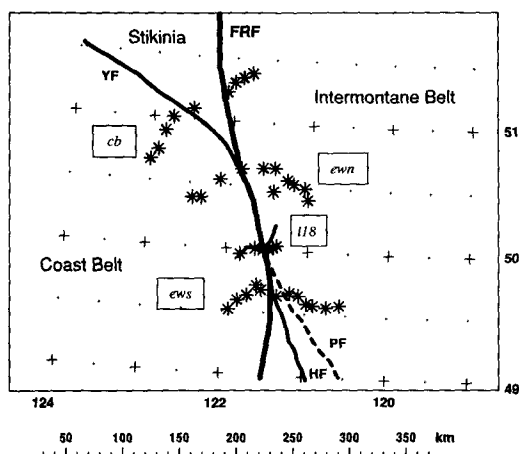


Figure 2. Locations of MT stations on four profiles crossing Fraser River fault: *cb*—Coast belt profile, *ewn*—east-west north profile, *118*—line 18 profile, *ews*—east-west south profile, *FRF*—Fraser River fault, *YF*—Yalakom fault, *HF*—Hozameen fault, *PF*—Pasayten fault. Also shown is location of line 18 seismic profile.

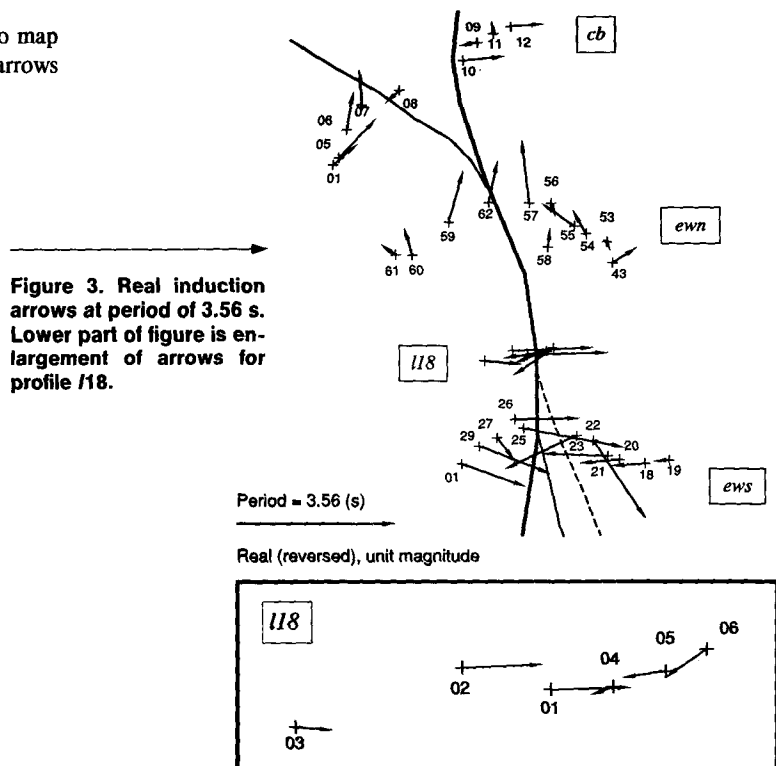


Figure 3. Real induction arrows at period of 3.56 s. Lower part of figure is enlargement of arrows for profile 118.

The variation along strike of the fault system is apparent in these images. In particular the phases at periods that sample the middle and lower crust (1–100 s) are different on either side of the Fraser River fault. This change, of 10° – 15° , occurs over a distance of <10 km. Model studies show that this rapid change cannot be accommodated for by a change in the upper crust on either side of the fault caused by the highly resistive Coast belt plutons, but argues for an abrupt change in the resistivity of the lower crust on either side of the fault. Accordingly, already from this data display we can deduce that the data are more consistent with a fault geometry represented by either A or B in Figure 1 than C or D. The difference for line *cb* is possibly due to the wedge of Stikine terrane that lies between the Fraser River and Yalakom faults. The implication from the lower phases observed is that the lower crust beneath this part of Stikinia is more resistive than that beneath either of the two bounding terranes.

Niblett-Bostick Depth Sections

To convert from period on the ordinate of the pseudosections to depth—i.e., to perform an “MT migration”—it is necessary to know the correct levels of the apparent resistivity curves. These levels are affected by distortions caused by local, small-scale structure and conductivity variations within the uppermost part of the crust. Such variations, while they are important for the complete study, are effectively “noise” on the regional data and must be removed. A first-order technique for leveling the MT data involves scaling the apparent resistivity curves such that they have the same averaged value at long periods. The value chosen for these data was $100 \Omega \cdot \text{m}$ at 100 s. The phases and scaled resistivities are then transformed from the period domain to the depth domain using the Niblett-Bostick transform (Jones, 1983).

The Niblett-Bostick depth sections are illustrated in Figure 5. These depth sections confirm the marked change in resistivity on either side of

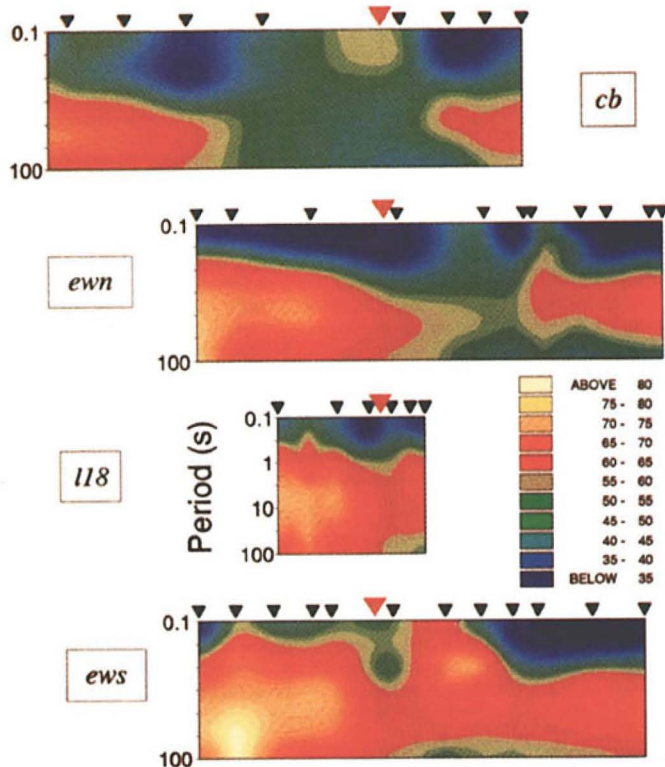


Figure 4. Determinant phase pseudosections of MT data from four Fraser River profiles. Inverted red triangles signify location of Fraser River. Blue areas denote resistive zones, green areas moderately conducting ones, and red and yellow areas highly conducting ones.

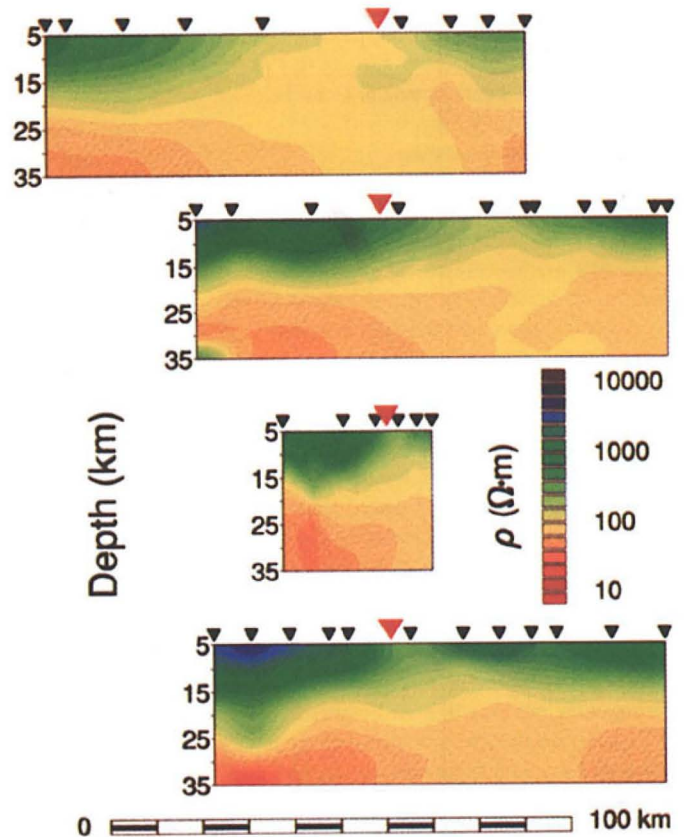


Figure 5. Niblett-Bostick depth sections for four Fraser River profiles. Inverted red triangle indicates location of Fraser River.

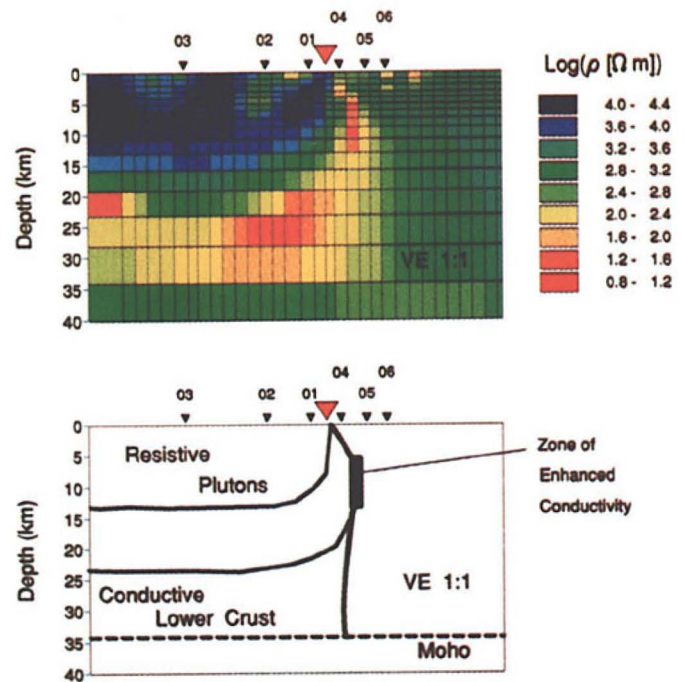


Figure 6. Two-dimensional model obtained by smooth inversion algorithm of data at nine periods from six sites along profile 118. Fraser River flows between sites 01 and 04. In color scale used, green and blue colors indicate resistivities $>1000 \Omega \cdot \text{m}$, yellows indicate $100 \Omega \cdot \text{m}$, and reds indicate $\sim 10 \Omega \cdot \text{m}$. Lower part of figure is cartoon interpretation of conductivity model derived.

the Fraser River fault with resistivities of the order of $30 \Omega \cdot \text{m}$ beneath the Coast belt and $80 \Omega \cdot \text{m}$ beneath the Intermontane belt. The lower crust beneath Stikinia is of higher resistivity ($>150 \Omega \cdot \text{m}$) than the lower crust beneath either the Intermontane or Coast belts.

Two-Dimensional Inversion

Given the complexity of the data from profiles *cb*, *ewn*, and *ews*, as indicated both by the MT responses and by the induction arrows (Fig. 3), a two-dimensional model may not be appropriate. In contrast, the data for profile *I18* are far simpler and are indicative of a dominantly two-dimensional conductivity structure; the induction arrows show a simple reversal, and Groom and Bailey (1989) decompositions indicate a north-south strike for much of the period range. What remains to be determined are the correct levels of the apparent resistivity curves. The inversion algorithm of deGroot-Hedlin (1991) solves simultaneously for the conductivity structure of the ground below the profile and for the level factors for each site. The code inverts for the smoothest conductivity distribution (minimizes the vertical and lateral conductivity gradients) that fits the observations. Other models could be found that also satisfy the data (to within the observational errors) but these models will have more variation in them. To include a priori information about the known thickness of the crust, a discontinuity in conductivity was permitted at a depth of 34 km to represent the Moho (Varsek et al., 1992).

The final model obtained is illustrated in Figure 6. Note the following features in the model, which are emphasized in cartoon form in Figure 6.

1. The upper crust to the west of the fault is more resistive (tens of thousands of $\Omega \cdot \text{m}$ compared to thousands) than that to the east. This is consistent with the presence of highly resistive plutons in the Coast belt. These plutons are modeled with a depth extent of 10–15 km.

2. There is a narrow vertical zone of enhanced conductivity, $\sim 10 \Omega \cdot \text{m}$, in the depth range 5–12 km below and slightly to the east of the Fraser River itself. Current concentration in this zone is responsible for the induction arrows observed here and on profiles *cb* and *ews*.

3. The conductivity of the lower crust changes markedly beneath the Fraser River fault across a zone that is at most 15 km wide. The depth to the conducting zone in the lower crust to the west of the fault is 20–23 km. This zone appears to terminate at the location of the Moho boundary. However, this may be a modeling artifact; the zone could equally be thinner and of higher conductivity.

4. The narrow mid-crustal zone and the lower crustal zone must be electrically connected. Models in which these zones are electrically isolated from each other do not fit the data as well.

CONCLUSIONS

The induction arrows (Fig. 3) clearly map enhanced current concentrations associated with the Fraser River, Yalakom, and Pasayten faults. Such current concentration was observed by Kirkwood et al. (1981) in the crustal-penetrating strike-slip Great Glen fault.

In a 275-km-long section of the Fraser River fault, MT data from four profiles are consistent in implying a rapid change in phase with lateral distance that must be due to a change in the conductivity of the lower crust at the location of the fault, with the more conducting strata to the west. It is not the purpose of this paper to discuss the reason for the observed enhanced conductivity beneath the Coast belt, but (1) a small increase in porosity (by 1%; Jones, 1992), (2) an increase in salinity of the pore fluid, or (3) an increase in partial melt would account for the lateral variation. This will be addressed in a subsequent paper.

Two-dimensional inversion confirmed this general result and also imaged a narrow vertical zone of enhanced conductivity associated with the fault itself that must be electrically connected to the lower crust. This zone lies slightly to the east of the surface trace of the fault.

These differing lower crustal conductivities on either side of the surface trace of the Fraser River fault suggest that the appropriate fault geometry is depicted by A or B in Figure 1 with penetration of the whole

crust. Such an interpretation is also compatible with the seismic observation of a 2 km “step” in the Moho just to the east of the fault and with the observed difference in structural style at lower crustal depths. In contrast, on interpreting their seismic data Varsek et al. (1992) rejected a high-angle crust-penetrating fault geometry in favor of geometry C mainly because of the continuity of mid-crustal reflectors beneath the fault's trace. The interpretation in this study implies that these mid-crustal reflectors are younger than the Fraser River fault, and, following Lemiszki and Brown (1988), the crust-penetrating geometry supports Price and Carmichael's (1986) proposal that the Fraser River–Straight Creek fault is part of an intracontinental transform-fault system.

Fluid-inclusion studies of δD values in the vein quartz of the Fraser fault system (Nesbitt and Muehlenbachs, 1991) indicate that the fluids are derived largely from isotopically evolved meteoric water. The lowest regional values for $\delta^{13}\text{C}$ were also observed in the fault system, indicating the presence of reduced carbon along the flow path. This suggests that the enhanced conductivity at mid-crustal depths may be due to organic carbon or graphite emplaced during upwelling in the fault zone of deeply penetrating surface waters.

Thus, the EM data suggest that (1) the fault penetrates the entire crust, (2) the fault has a subvertical geometry, (3) there is a step change in electrical conductivity, by half an order of magnitude, in the lower crust on crossing the fault, and (4) the fault was, and may still be, a conduit for escape of deeply penetrating meteoric waters.

REFERENCES CITED

- Bois, C., Cazes, M., Damotte, B., Galdéano, A., Hirn, A., Mascle, A., Matte, P., Raoult, J.F., and Torrelles, G., 1986, Deep seismic profiling of the crust in northern France: The ECORS project, in Barazangi, M., and Brown, L., eds., *Reflection seismology: A global perspective*: American Geophysical Union Geodynamics Series, v. 13, p. 21–29.
- Coleman, M.E., and Parrish, R.R., 1991, Eocene dextral strike-slip and extensional faulting in the Bridge River terrane, southwest British Columbia: *Tectonics*, v. 10, p. 1222–1238.
- deGroot-Hedlin, C., 1991, Removal of static shift in two dimensions by regularized inversion: *Geophysics*, v. 55, p. 1613–1624.
- Groom, R.W., and Bailey, R.C., 1989, Decomposition of magnetotelluric impedance tensor in the presence of local three-dimensional galvanic distortion: *Journal of Geophysical Research*, v. 94, p. 1913–1925.
- Jones, A.G., 1983, On the equivalence of the “Niblett” and “Bostick” transformations in the magnetotelluric method: *Journal of Geophysics*, v. 53, p. 72–73.
- , 1992, Electrical properties of the continental lower crust, in Fountain, D.M., et al., eds., *The lower continental crust*: Amsterdam, Elsevier (in press).
- Keen, C.E., and ten others, 1986, A deep seismic reflection profile across the northern Appalachians: *Geology*, v. 14, p. 141–145.
- Kirkwood, S.C., Hutton, V.R.S., and Sik, J., 1981, A geomagnetic study of the Great Glen fault: *Royal Astronomical Society Geophysical Journal*, v. 66, p. 481–490.
- Lemiszki, P.J., and Brown, L.D., 1988, Variable crustal structure of strike-slip fault zones as observed on deep seismic reflection profiles: *Geological Society of America Bulletin*, v. 100, p. 665–676.
- McCaig, A.M., 1988, Deep fluid circulation in fault zones: *Geology*, v. 16, p. 867–870.
- McGeary, S., 1989, Reflection seismic evidence for a Moho offset beneath the Walls Boundary strike-slip fault: *Geological Society of London Journal*, v. 146, p. 261–269.
- Nesbitt, B.E., and Muehlenbachs, K., 1989, Origins and movement of fluids during deformation and metamorphism in the Canadian Cordillera: *Science*, v. 245, p. 733–736.
- , 1991, Stable isotopic constraints on the nature of the syntectonic fluid regime of the Canadian Cordillera: *Geophysical Research Letters*, v. 18, p. 963–966.
- Parkinson, W.D., 1959, Direction of rapid geomagnetic fluctuations: *Royal Astronomical Society Geophysical Journal*, v. 2, p. 1–14.
- Price, R.A., and Carmichael, D.M., 1986, Geometric test for Late Cretaceous–Paleogene intracontinental transform faulting in the Canadian Cordillera: *Geology*, v. 14, p. 468–471.
- Varsek, J.L., Cook, F.A., Clowes, R.M., Journeay, J.M., Monger, J.W.H., Parrish, R.R., Kanasevich, E.R., and Spencer, C.P., 1992, Lithoprobe crustal reflection structure of the southern Canadian Cordillera II: Coast Mountains transect: *Tectonics* (in press).

ACKNOWLEDGMENTS

The MT data were acquired by Phoenix Geophysics (Toronto) Ltd. We thank the Phoenix crew, in particular George Elliot, for assistance in obtaining high-quality MT data; Catherine deGroot-Hedlin for providing the two-dimensional inverse code; and Fred Cook, Randy Parrish, and Jim Monger for their comments on an earlier draft. Geological Survey of Canada Contribution No. 28491. Lithoprobe publication no. 285.

Manuscript received September 18, 1991

Revised manuscript received March 10, 1992

Manuscript accepted March 12, 1992